A TRANSGENIC MOUSE MODEL OF MERKEL CELL VIRUS SMALL TUMOR ANTIGEN

by

Stefan Nicholas Lukianov

Bachelor of Science in Biochemistry and Molecular and Cellular Biology

University of Maine, 2006

Submitted to the Graduate Faculty of the

Program in Integrative Molecular Biology and

University of Pittsburgh School of Medicine

In partial fulfillment of the requirements for the degree of

Master of Science in Molecular Biology

University of Pittsburgh

2013

UNIVERSITY OF PITTSBURGH

SCHOOL OF MEDICINE

This thesis was presented by

Stefan Nicholas Lukianov

It was submitted on

October 1, 2013

and approved by

Patrick S. Moore, PhD, Microbiology and Molecular Genetics, Thesis Advisor

Jeffrey Hildebrand, PhD, Biological Sciences, Program Director

A TRANSGENIC MOUSE MODEL OF MERKEL CELL VIRUS SMALL TUMOR ANTIGEN

Stefan Nicholas Lukianov, BS

University of Pittsburgh, 2013

Merkel cell carcinoma (MCC), a primary cutaneous neoplasm, originates in the mechanoreceptor Merkel cells in the basal layer of the epidermis. Risk factors include UV exposure, advanced age and immunosuppression, suggesting an infectious etiology. MCC incidence in the US is rising, with approximately 1500 cases per year. The non-enveloped, double-stranded DNA Merkel cell polyomavirus (MCV) is responsible for approximately 80% of MCC cases. The virus was discovered by subjecting MCC tissue samples to digital transcriptome subtraction, in which mRNA is isolated, the human transcripts subtracted *in silico* and the remaining transcripts compared to viral sequences.

MCV expresses differentially spliced Large (LT), Small (sT) and 57 kT tumor antigens from the T antigen early locus, similar to other polyomaviruses such as SV40. Both LT and sT are critical for transformation. LT is a helicase responsible for replication of the viral genome, however in integrated viral genomes it is either truncated or mutated to eliminate its replicative functions. sT contributes to transformation via hyperphosphorylation and inhibition of the cap-dependent translation inhibitor 4E-BP1. The function of 57 kT remains unknown. Knockdown of LT induces necroptosis of MCV-positive MCC cells, whereas sT expression in rodent Rat-1 cells is transformative.

Being that sT is the transformative agent in rodent cells, it would be of interest to develop a mouse model expressing sT in a tissue-specific manner to determine whether tumor formation occurs. Indeed, several mouse models of SV40 T antigen have been developed over the past decades, each resulting in tissue-specific tumor formation. We developed a MCV sT transgenic mouse model, in which a lox-stop-lox sT is expressed via an ER-inducible Cre gene under the control of the ubiquitin promoter. Upon tamoxifen-induced MCV sT expression, ER-Cre-positive mice demonstrate severe weight loss, ruffled fur and a hunched posture, necessitating euthanasia. Western blotting reveals sT expression in several tissues, whereas TUNEL staining shows significant cell death. While we were unable to observe transformation, we believe this drastic phenotype demonstrates the validity of our MCV sT transgenic mouse model and warrants further investigation into the mechanism of death.

Table of Contents

List of Figures

Acknowledgements

I would first like to thank my mentors Dr.'s Patrick Moore and Yuan Chang. They graciously accepted me into their lab and provided the opportunity to learn and grown in a supportive and intellectually satisfying environment. Were it not for them, I would not have acquired the extensive technical and conceptual knowledge that I now possess. I am a significantly better scientist for having been in their lab. I would also like to thank the director of PIMB, Dr. Jeffrey Hildebrand. During difficult times in my graduate tenure he was extremely helpful and compassionate. He invested great effort in ensuring that I received the most out of the program. I would also like to thank Susanna Godwin and Jennifer Walker for their extensive administrative help and answering my often foolish questions. I would not have been able to navigate the complexities of our educational system without them. My thanks also go out to my thesis committee of Dr.'s Tom Smithgall, Neil Hukriede, Alan Wells and Lin Zhang. Their constructive input and advice were more than welcome additions to my intellectual growth.

My family provided indispensable support and love during my time away from them in Pittsburgh. I have always been able to confide in them and they have always reassured and guided me with gentleness and attentiveness. I am indebted to them on more levels than I can adequately express. Finally, I would like to thank God for being with me always and helping me to make what I believe to be the appropriate decisions at each moment. His eternal love and grace are my life support. Praise be to You, O Lord.

1.0 MERKEL CELL CARCINOMA

Cyril Toker first described Merkel cell carcinoma (MCC), an aggressive and rare form of skin cancer, in 1972 (**Fig 1**)(1). This primary cutaneous neoplasm of the dermis forms sheets, nests or trabecular and anastomosing aggregates (2). Invasion of the overlying epidermis is rare, but entry into the subcutis does occur. MCC cells have granular or vesicular round, oval nuclei, along with syncytial-appearing cytoplasm, small nucleoli and increased mitotic activity. There is variance on a case-by-case basis for intratumoral necrosis and inflammatory infiltration. The cytoplasm contains dense-core, membrane bound structures, and the cells express chromogranin, synaptophysin and other neuropeptides, thus characterizing them as cutaneous neuroendocrine carcinomas (3). The perinuclear space contains cytokeratin intermediate filaments that form fibrous bodies through oligomerization. Indeed, cytokeratin 20 staining is the primary marker used to diagnose MCC (2). Histologically, MCCs develop as pure lesions, though occasionally there is involvement of ectodermal and mesodermal neoplasms (2).

In 2001, the incidence of MCC was 4.4 cases per million in the US (4). The five-year survival rate for localized tumors was 75%, whereas that for disseminated tumors was 25% (5). Clearly, MCC is rare, but the high mortality rate is due to the aggressiveness of the neoplasm. Those most at risk are the elderly, the immunosuppressed such as transplant and AIDS patients, and those exposed to UV light (2, 6, 7). These factors suggest that MCC has an infectious etiology, i.e. viral (2).

Figure 1. Merkel cell carcinoma lesion. Located on the arm of the patient. Note the nodular, red and raised clinical appearance. Adapted from (2).

2.0 MERKEL CELL POLYOMAVIRUS

To identify the putative infectious virus for MCC, Feng et al. dissected four MCC tumor samples and isolated the mRNA (8). To distinguish viral from human mRNA, the investigators used digital transcriptome subtraction. In this method, mRNA is reverse transcribed into a cDNA library then subjected to deep sequencing to produce a sample library. Next, using the databases made available by the Human Genome Project, an *in silico* subtraction of all human sequences is performed. The remaining candidate transcripts are then compared to viral sequences at low stringency to examine any homology. With this method, Feng et al. identified a transcript possessing 54% homology to the tumor antigen of the African lymphotropic green monkey polyomavirus. The viral genome was then sequenced and dubbed Merkel cell polyomavirus (MCV), a nonenveloped double-stranded DNA virus (**Fig 2**).

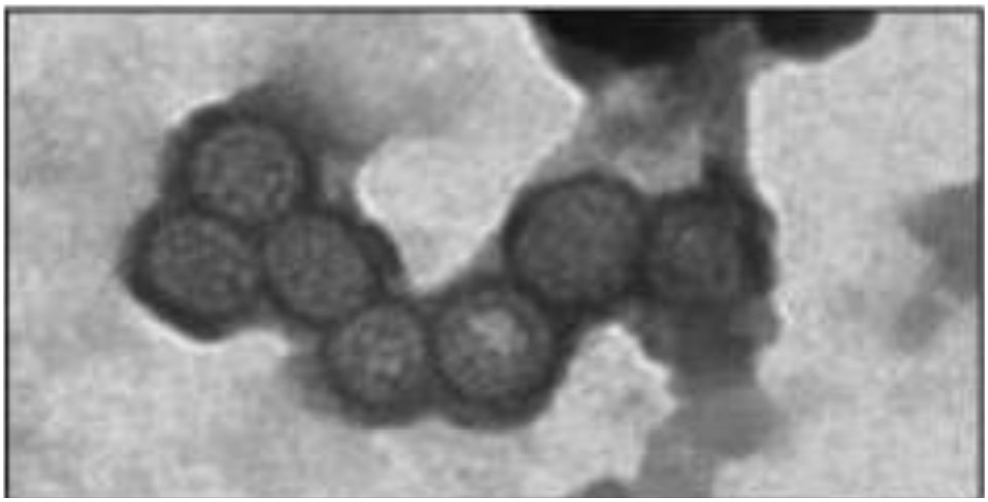

Figure 2. Merkel cell polyomavirus particles. Whole genome transfected into 293 cells for production. Adapted from (20).

2.1 PREVALENCE OF MCV

In a later study, 8 of 10 MCC tumors tested positive for the presence of the MCV genome, with some cells having up to 48 copies of the virus (9). Another 27 published studies of 819 MCC patients from North America, Europe and Asia in 2010 found 634 (77.4%) of tumors to be MCV positive (2). Both primary tumors and metastases displayed clonal integration of the viral genome (9, 10). In different MCCs, the viral genome integrates at insertion sites throughout the host genome as head-to-tail concatemers, suggesting that tumors harboring MCV are accidental in origin (9, 10-13). Interestingly, several tissues from healthy and non-MCC patients have low copy numbers of the MCV genome, indicating that MCV is a normal component of skin flora at different body sites (2, 8, 9, 14). Using serology with antibodies against the viral structural protein VP1, one study found that 59% of control subjects from the general population harbored MCV (15). Another study discovered that seroprevalence increases with age, with 80% of North American blood donors at age 50 showing evidence for MCV exposure (16).

2.2 MCV GENOME STRUCTURE

The viral genome of MCV is 5,387 bp with a noncoding-regulatory region (NCRR) dividing an early and late coding region (**Fig 3**)(2, 8). The NCRR contains the 71-bp viral origin. The origin contains an AT-rich sequence that aids in DNA melting, as well as 8 copies of a GAGGC pentanucleotide sequence. The NCRR regulates early and late viral gene expression using regulatory sequences and bidirectional transcriptional promoters. The MCV early region contains the tumor (T) antigen locus. From this locus, large (LT), small

(sT) and 57-kT tumor antigens are expressed via differential splicing. The late region encodes the structural capsid proteins VP1, VP2 and VP3 expressed after viral replication.

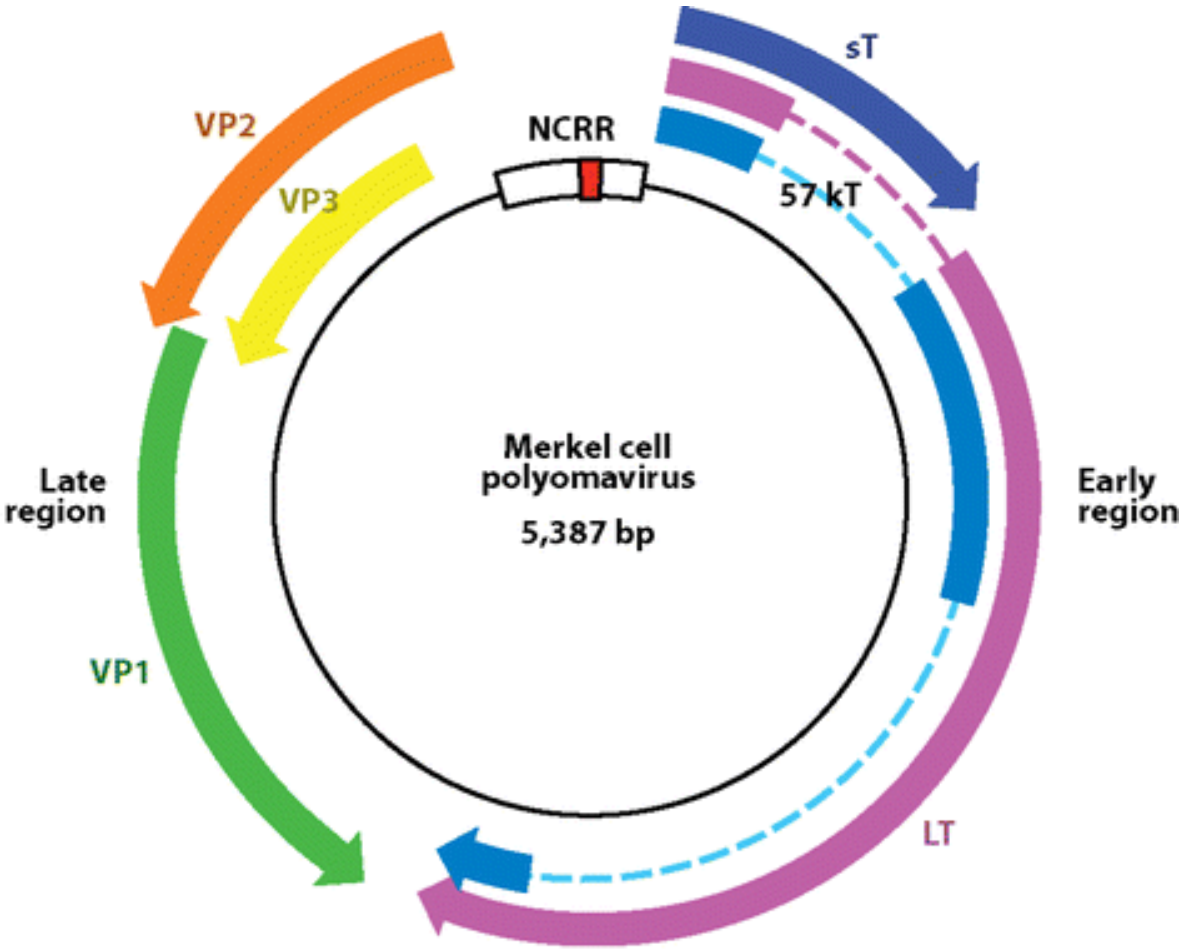

Figure 3. MCV genome structure. The genome is 5,387 bp long. The noncoding regulatory region (NCRR) contains early and late promoters from which bidirectional transcription occurs. The red band in the NCRR indicates the viral origin, a 71 bp contiguous sequence bound by the large tumor antigen (LT). The T antigen locus comprises the early region, whereas the VP1, VP2 and VP3 proteins reside in the late region. Adapted from (2).

2.3 MCV TUMOR ANTIGENS

MCV LT contains several domains including a conserved region 1 (CR1), DnaJ, a nuclear localization signal (RKRK), Rb-binding (LXCXE), origin binding domain (OBD), Zinc finger C_2H_2, Leucine zipper, ATPase domain and helicase domain (**Fig 4**). MCV sT contains CR1, DnaJ and a PP2A binding site included by differential splicing (**Fig 4**). 57-kT contains CR1, DnaJ and the Rb-binding domain (**Fig 4**). As indicated by its domain architecture, LT is involved in viral replication. Interestingly, in MCC cells the region of the T antigen gene encoding MCV LT has missense mutations or deletions that eliminate the replication motifs at the C-terminus, such as the OBD or helicase domain, thus viral DNA replication is lost (17). Other mutations occur in the viral origin or VP1 capsid protein (18,19). However, the mutations do not interfere with N-terminal domains, such as the Rb-binding domain nor sT domains. Accordingly, MCV LT from different MCC tumors varies in size depending on the site of mutation (9).

It is speculated that the active viral replication results in lysis and cell death, thus providing strong tumor selection of the above MCV LT mutations (13). DNA replication induced by full-length MCV LT at newly integrated sites results in replication-fork collisions and breakage of the DNA (17). The reason for the rarity of MCC despite the prevalence of MCV infection may be due to integration of the viral genome and MCV LT mutation being independent events, making the combination less probable. Functionally, tumor-derived MCV LT is unable to induce transformation in soft agar colony formation, focus formation nor cell growth in low serum (21). This is in contrast to the ability of MCV sT to fully transform rodent fibroblasts that is unenhanced by expression of MCV LT. However, MCV LT is necessary for the survival of MCC-derived cell lines, and this depends

on a functional Rb-binding domain, the mutation of which abolishes Rb binding (17, 22). Moreover, knockdown of MCV LT results in nonapoptotic cell death of MCV positive MCC cells (12). MCV LT knockdown in MCC cells was also found to decrease mRNA and protein levels of the anti-apoptotic gene survivin, which is highly upregulated in MCV-positive MCC (23). Additionally, ectopic expression of MCV LT in non-MCC BJ primary cells increased survivin expression. An intact Rb-binding domain was required for this induction. Finally, YM155, a small molecule inhibitor of survivin, inhibits MCV-positive MCC growth (20). Collectively, these results point to a possible molecular mechanism by which MCV LT contributes to tumorigenesis via survivin.

Whereas the function of 57 kT remains unknown, sT is able to fully transform Rat-1 rodent fibroblasts (21). Knockdown of sT in MCV-positive MCC cells arrests proliferation but does not result in cell death, as knockdown of MCV LT does. Mutation of the PP2A binding site in sT does not abolish its oncogenic activity, suggesting that this activity is independent of sT binding to the cellular phosphatase PP2A. sT does, however, activate cap-dependent translation by promoting hyperphosphorylation of 4E-BP1, a target of the Akt-mTOR pathway, through an unknown mechanism. Phosphorylation of 4E-BP1 by mTOR releases eIF4E, a translation initiation factor. eIF4E is then able to bind 7-methylguanosine-capped mRNA for ribosomal assembly. Thus, MCV sT-induced hyperphosphorylation of 4E-BP1 likely deregulates cap-dependent translation and enhances transformation. Despite the fact that LT does not enhance sT-induced transformation of rodent fibroblasts, cooperation likely exists between

T antigen isoforms as expression of sT in MCC cells that have a repressed T antigen locus does not rescue growth.

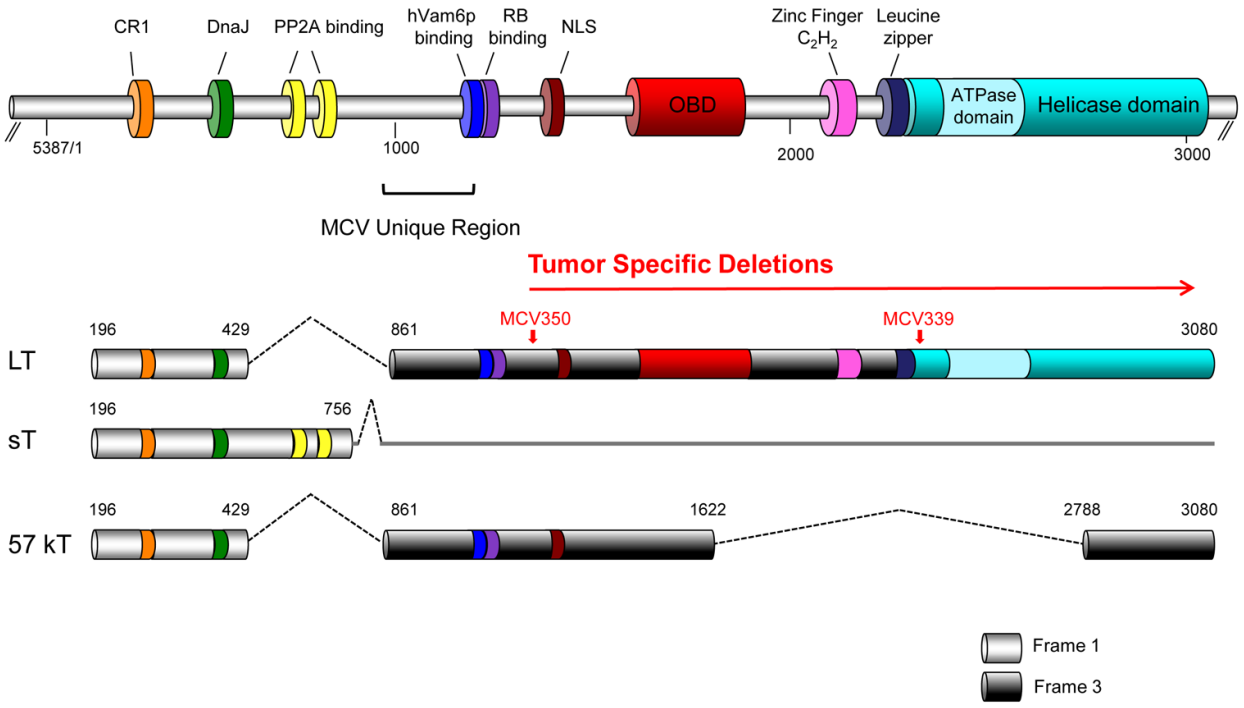

Figure 4. **MCV tumor antigens**. Alternative splicing generates the three tumor antigens. Domain structure for each is shown in various colors. Mutation sites for two MCV strains (MCV350 and MCV 339) are indicated by red arrows over LT. Adapted from (20).

3.0 SV40 T ANTIGEN TRANSGENIC MOUSE MODELS

Given that MCV sT is the transformative agent in rodent fibroblasts, it would be of significant interest to "scale-up" the experimental system to a mouse model to determine whether a similar phenotype is observed, i.e. tumor development in a tissue specific manner. Such research would provide greater mechanistic and clinical insight into MCV biology and MCC itself. Several successful and informative mouse models of Simian vacuolating virus 40 (SV40) T antigen have been developed over the past decades, thus the idea is not without precedent (24).

3.1. SV40 T-ANTIGEN

For SV40 to use the cellular machinery for its replication, and thereby induce transformation, the cells must re-enter S phase (24). This enables the cells to grow in environments that are not permissive to untransformed cells, such as in the absence of serum. Transformed cells can form dense, multilayered foci, are anchorage independent and can induce tumors in immune-compromised mice. SV40 LT is responsible for viral replication, transcriptional regulation and virion assembly, and is both necessary and sufficient to induce transformation, as opposed to MCV LT. SV40 sT contributes to transformation by binding PP2A. SV40 LT contains five structural domains and interacts with multiple binding partners (**Fig 5**). The most important interactions are with the pRb family of proteins via an LXCXE motif and p53 via the ATPase domain. Binding and

inactivation of pRbs by SV40 LT induces cellular proliferation, whereas binding and inactivation of p53 blocks the resulting apoptotic response.

3.2 BRAIN

The most studied mouse model of SV40 T antigen-induced transformation in the brain is in the choroid plexus epithelium (CPE) (24). This tissue produces and filters cerebrospinal fluid to protect the brain from immune cells, metabolic waste and foreign substances. Expression of SV40 T antigen in the CPE rapidly induces tumor formation independent of sT. The mice eventually die around 1 month of age (25, 26). Blockage of the pRb pathway is essential for transformation. Normally, the re-entry into S phase and E2F1 upregulation triggered by pRb disruption would lead to a p53-mediated apoptotic response, however SV40 T antigen also binds and inactivates p53 to promote survival of the rapidly proliferating cells.

3.3 INTESTINE

SV40 T antigen has been expressed in various tissues of the small intestine, including the endocrine cells (27-29), Paneth cells (30), goblet cells (31), smooth muscle cells (32), and enterocytes (33-35). This usually results in quiescent cells re-entering S phase, but in some cases involution and/or apoptosis occurs (30,31). Dysplasia may also occur (33,36). Interestingly, a truncated amino-terminal mutant of SV40 T antigen that retains pRb binding but lacks p53 binding is still sufficient to drive S phase re-entry in

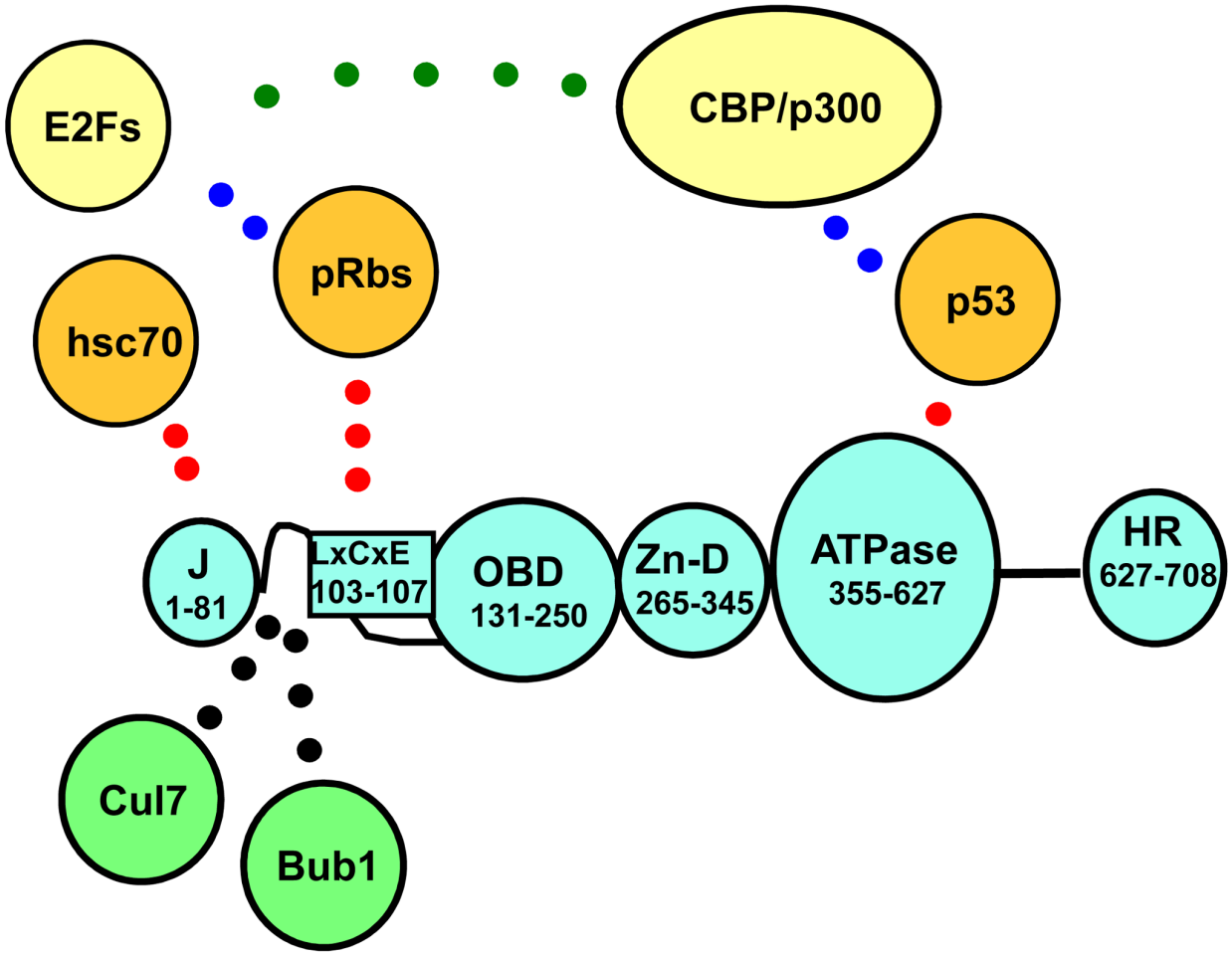

Figure 5. SV40 Large T antigen structure and interactions. SV40 LT contains a J domain, an LXCXE motif, an origin binding domain (OBD), a zinc-finger domain (Zn-D), an ATPase domain (ATPase) and a host –range domain (HR). It's interaction with the pRbs and p53 are the primary method by which SV40 LT induces transformation. Adapted from (24).

enterocytes and hyperplastic intestines, indicating that p53 does not play a role (37). However, disrupting the interaction with pRb or the J domain abrogates the mutant phenotype (37-39). Finally, increased steady state levels of the transcription factors E2F2 and E2F3 were also observed in enterocytes induced to proliferate by SV40 T antigen (37).

3.4 EYE

Expression of SV40 T antigen in the retina of transgenic mice induces tumors similar to retinoblastoma in humans (40). In the ocular lens, T antigen induces tumorigenesis and decreases expression of differentiation markers, whereas a truncated amino terminal mutant induces proliferation and apoptosis, presumably due to the absence of the p53 binding site, resulting in microphtalmia, microlentia and lens ablation (41). Disruption of pRb is necessary for induction of proliferation in the fiber cells of the lenses, but sT is not required (42,43).

3.5 PANCREAS

SV40 T antigen has also been expressed in the β-cells in the islets of the pancreas in RIP-Tag2 mice (44). These cells re-enter S phase and exhibit hyperplasia and dysplasia. All p53-induced apoptosis is effectively suppressed in this system (45). Additional mutations, such as activation of the survival factor IGF2, are necessary to promote tumorigenesis (44, 46). In acinar cells, carcinomas and metastasis are induced by expression of both SV40 LT and sT (47-50). Truncated amino terminal T antigen is also sufficient to generate this

phenotype, indicating that disruption of p53 is unnecessary, and sT is also dispensable (51). Finally, insulinomas and lymphomas are observed when T antigen is expressed in the endocrine cells of the pancreas (28).

4.0 A TRANSGENIC MOUSE MODEL OF MCV ST

4.1 BACKGROUND AND SIGNIFICANCE

As previously mentioned, MCV sT is capable of transforming rodent fibroblasts on its own (21). This activity is independent of its PP2A binding site, but possibly occurs via an sT-mediated increase in cap-dependent translation due to hyperphosphorylation and inhibition of the translation inhibitor 4E-BP1. It is unknown, however, whether sT is able to transform cells *in vivo*. A transgenic mouse expressing MCV sT would be a more physiologically relevant model of MCC that would provide insight into MCV biology in a living host.

4.2 HYPOTHESIS

My hypothesis is that tissue-specific expression of MCV sT will induce tumorigenesis in a transgenic mouse model. MCV sT should be able to perform its oncogenic function in a living rodent similar to its action in rodent fibroblasts because both models share molecular characteristics.

4.3 SPECIFIC AIM: GENERATE A TRANSGENIC MOUSE MODEL OF MCV ST

To determine whether MCV sT can transform cells in an *in vivo* context as well as *in vitro*, a transgenic mouse model expressing sT in a tissue specific manner will be

developed. The cre-lox system is ideal for generating such a model. This method inserts the sT gene under the control of a constitutive promoter into a specific locus in the mouse genome. Between the gene and the promoter is a "stop cassette" flanked by loxP sites that prevents expression of sT until excision of the stop cassette by cre recombinase. Cre is expressed under the control of a tissue-specific promoter, so excision, and sT expression, will only occur in cre-expressing tissues. Subsequently, sT expression in the tissue of interest can be determined using western blotting, and tumor formation can be observed.

5.0 EXPERIMENTATION

5.1 GENERATION OF A TRANSGENIC MCV ST KNOCK-IN MOUSE

5.1.1 *Rosa26* targeting and cre recombination

To study the effects of MCV sT *in vivo*, we first enlisted GenOway to develop a transgenic MCV sT knock-in mouse for us. GenOway performed all experimental steps in this development, and then sent the finished transgenic heterozygous mice to us (see section 5.2 onwards for our experiments). The initial step was the selection of the *Rosa26* locus as the target for the sT transgene. This locus was discovered in a promoter gene trap strain, *Rosa26-β-geo* (52,53). Due to the ubiquitous expression of this locus it is often used for transgene insertion. Typically, a STOP cassette flanked by LoxP sites (floxed) is placed between the transgene and the promoter to enable Cre recombinase-dependent expression. Another reason the *Rosa26* locus is desirable is because it has an open chromatin structure, permitting efficient homologous recombination in embryonic stem cells.

Some further advantages of GenOway's *Rosa26* knock-in technology are 1; a preselected integration site, 2; analysis can be performed *in vivo* on a single transgenic line, 3; high homologous recombination frequency is attainable at the *Rosa26* locus, 4; GenOway has a ready-to-use targeting vector, 5; the recombination frequency has been optimized by GenOway, and 6; generation of ES cell clones with transgene insertion is guaranteed. Some disadvantages are 1; being that the *Rosa26* locus is neutral, selection media can not be used, therefore an excisable neomycin resistance cassette must be incorporated into the

transgene construct that may interfere with transgene expression, and 2; impaired breeding in homozygous *Rosa26* knock-in mice.

5.1.2 Targeting vector construction

GenOway's final targeting vector PAM1-HR was constructed through conventional molecular biological methods. The initial step was insertion of a 571 bp HincII/XhoI sT fragment into the G194 vector digested with SmaI/XhoI. This generates the 3516 bp plasmid PAM1-CDS. Next, a 585 bp XhoI/SgrA1 digested sT fragment is isolated from PAM1-CDS and subcloned into the ARC1-pA vector digested with PshA1/XmaI. The resulting 15648 bp plasmid was termed PAM1-HR. Validation was performed through restriction analysis and partial sequencing of the coding exons, junction between selection cassettes and homology arms, positive and negative selection cassettes, and junctions between the plasmid backbone and homology arms.

The sT transgene was placed under the control of the CAG promoter (**Fig 6**). This is a combination of the CMV immediate early enhancer and the chicken β-actin promoter that demonstrates strong and ubiquitous expression. The floxed STOP cassette was placed between the CAG promoter and sT transgene, which effectively abrogates transcription. Exxpression of the cre recombinase gene under the control of a tissue-specific promoter leads to excision of the STOP cassette and tissue-specific expression of the sT transgene. Also between the CAG promoter and STOP cassette is a neomycin resistance gene to serve as a positive selection marker that can be removed via cre expression.

5.1.3 Homologous recombination in embryonic stem cells

PAM1-HR was linearized by digestion with AscI, and then subjected to phenol/chloroform extraction and ethanol precipitation for isolation and purification. 40 µg of linear DNA was then electroporated into $5x10^6$ ES cells derived from a C57BL/6 mouse strain at 200 V and 500 µF. After 48 hours positive selection with 200 µg/mL G418 was begun, and colonies were chosen based on cell growth and morphology. After three rounds of electroporation, 1577 clones were isolated and amplified on duplicate 96 well plates. One plate was frozen at -80 °C, while the other was used for genomic DNA isolation and screening for homologous recombination using PCR and southern blotting.

5.1.4 PCR, Southern blotting and sequencing to detect homologous recombination in ES cells

Initially, PCR screening was used to determine whether homologous recombination had occurred at the 5' end of ES cell genomic DNA. The reverse primer GX6044 (5'-GCAGTGAGAAGAGTACCACCATGAGTCC-3'), binding in the short homology arm upstream of the hGHpA, and the forward primer GX6043 (5'- AAGACGAAAAGGGCAAGCATCTTCC -3'), binding upstream of the targeting vector homology sequence, were used. The expected product size indicating homologous recombination is 1870 bp. 18 positive clones were isolated in the initial screening.

For southern blotting to detect 5' homologous recombination, ES cell genomic DNA was digested with AvrII and probed with the ROSA-5E-B probe that hybridizes upstream of the targeting vector homology sequence. The wild-type locus will generate a fragment of

5273 bp, whereas with transgene insertion the fragment size will be 11470 bp. 15 out of the 18 PCR verified clones were found to have 5' homologous recombination events. For southern blotting to detect 3' homologous recombination, ES cell genomic DNA was digested with EcoRV and probed with the ROSA-31-W probe that hybridizes in the targeting vector's 3' homology sequence. The wild-type locus will generate a fragment of 9248 bp, whereas with transgene insertion the fragment size will be 13091 bp. The same 15 clones identified using 5' southern blotting were identified using 3' southern blotting. As a final validation, the MCV sT transgene in these 15 clones was sequenced and 13 were found to possess the transgene.

5.1.5 Chimera generation by blastocyst injection of ES cell clones and mating

Pregnant C57BL/6 were used as the donors for blastocysts. After injection of the ES cell clones, blastocysts were implanted into OF1 pseudo-pregnant females. The inner cell mass of 3.5 day-old embryos, the blastocyst stage, is composed of ES cells. Due to the pluripotency of ES cells, they are able to colonize a host blastocyst post-injection and contribute to every cell lineage, including germline. As aforementioned, the ES cells in this experiment have a C57BL/6 background, which generates black-coat color. The host blastocysts, however, are from an albino C57BL/6J-Tyrc-2J/J strain. Therefore, the injected blastocysts are composed of two cell types from animals with different coat colors, and thus the patches of black and white fur on the resulting mice can be used to monitor chimerism. 7 males with greater than 50% chimerism were generated from injected blastocysts.

These male chimeras were mated to C57BL/6 females to determine if the recombined ES cells contributed to the germ layer. Tail biopsies were taken from agouti generation F1 pups for DNA isolation. PCR genotyping was then performed as described above for the recombined ES cells to determine if the sT transgene was present. Out of 63 pups tested, two females and one male harbored the transgene. Southern blot analysis as described above was also performed on the male and one female and confirmed that the pups were heterozygous for the transgene.

5.2 BREEDING OF MCV ST TRANSGENIC MICE

5.2.1 Generation of sT homozygotes

Upon receipt of the sT heterozygotes from GenOway, breeding was begun to generate sT homozygotes. PCR was used to distinguish wild-type, heterozygote and homozygote offspring using genomic DNA isolated from ear notches. This consisted of two primer pairs, one recognizing the endogenous *Rosa26* locus (forward: CAATACCTTTCTGGGAGTTCTCTGC, reverse: CTGCATAAAACCCCAGATGACTACC, product of 300 bp) and another recognizing the knock-in locus (forward: ACCGCCCCACACTTATTG, reverse: GCTTCACTTGCATCTCTTCTG, product of 2,100 bp). Out of two litters, six sT homozygotes were obtained.

5.2.2 Breeding of sT homozygotes to UBC-ER-Cre heterozygotes

Once sT homozygotes were obtained, they were bred to B6.Cg-Tg(UBC-cre/ERT2)1Ejb/J heterozygotes (Jackson Labs #008085). These mice express the cre

recombinase fused to the estrogen receptor and under the control of the ubiquitin promoter, which is expressed in all tissues. Upon introduction of an estrogen analog, the ER-cre translocates into the nucleus to catalyze recombination of loxP sites. This enables excision of the STOP cassette located between the sT transgene and CAG promoter, thereby inducing sT expression in all tissues (**Fig 6**). PCR using primers specific to the cre transgene (forward: GCG GTC TGG CAG TAA AAA CTA TC and reverse: GTG AAA CAG CAT TGC TGT CAC TT, product of 100 bp) was used to identify offspring carrying the UBC-ER-cre transgene.

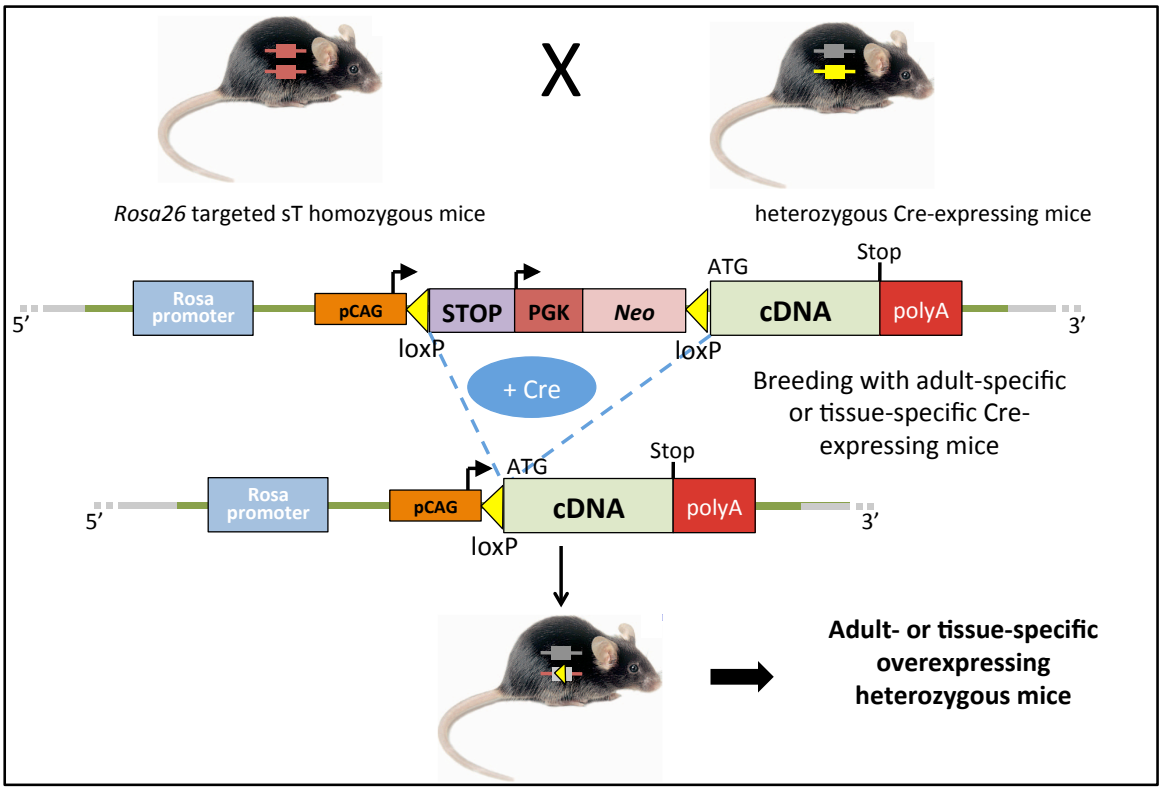

Figure 6. MCV sT transgene and cre breeding scheme. The MCV sT transgene is knocked-in at the *Rosa26* locus and is under the control of the constitutive pCAG promoter, with a floxed STOP cassette including a neomycin resistance gene between the two to prevent sT expression. Upon tissue-specific expression of cre when sT homozygotes are bred to cre heterozygotes, the STOP cassette is excised, inducing expression of sT.

5.3 TAMOXIFEN INJECTIONS

Tamoxifen, an estrogen analog converted to 4-hydroxytamoxifen in the liver, was purchased from Sigma. It was dissolved in corn oil (Sigma) at 65°C for 1 hour, filter sterilized, and injected intraperitoneally into 4 week old genotyped mice from crosses between sT homozygous females and UBC-ER-cre heterozygous males. A total of 11 mice, six UBC-ER-cre negative and 5 UBC-ER-cre positive from two separate litters, were injected once at 0.2 mg/g body weight each day for three days. One UBC-ER-cre positive mouse was not injected with tamoxifen as a negative control. Injected mice were weighed on days zero and three (**Fig 7**). Any mouse having a 20% loss in body weight was sacrificed by carbon dioxide asphyxiation followed by cervical dislocation. We then harvested the brain, heart, intestines, kidneys, liver, lungs, spleen and muscle. Pieces of each organ were either flash frozen on dry ice and stored at -80°C for western blots or fixed in 10% buffered formalin for slide preparation.

5.4 WESTERN BLOTS OF TISSUE SURVEY FOR ST EXPRESSION

Organ samples stored at -80°C were thawed and lysis buffer (50 mM Tris-HCl, 150 mM NaCl, 1% Triton X-100, with Roche Complete Mini protease inhibitors) added. Samples were pulverized with a pestle, sonicated, centrifuged at 10 krpm and lysate collected. Protein concentration was measured using the Biorad DC protein assay kit with BSA standards and a Biotek Synergy 2 plate reader. For western blots to detect sT expression in the various tissues for each mouse, 50 µg protein was loaded onto a 12% polyacrylamide gel and run at 15 mA until the dye front reached the bottom of the gel. Protein was then

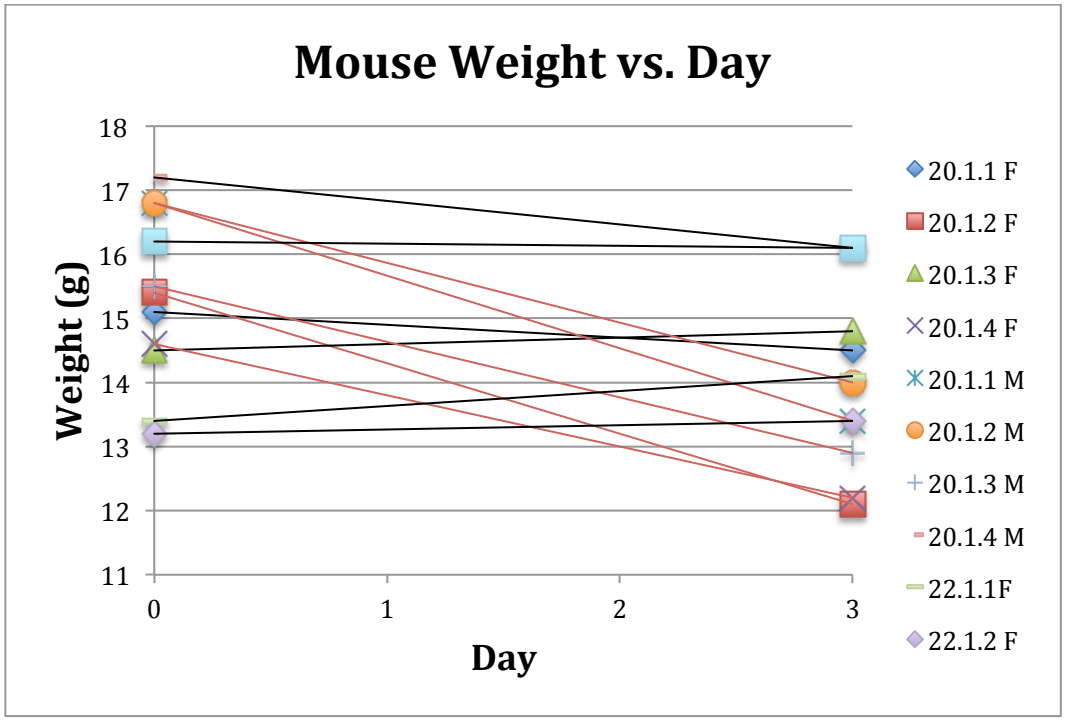

Figure 7. Mouse weights in response to tamoxifen injections. Black lines represent UBC-ER-cre negative mice, whereas red lines represent UBC-ER-cre positive heterozygotes. Mice were injected at 0.2 mg/g body weight once a day over 3 days, then sacrificed on day 3 and organs harvested.

transferred to a nitrocellulose membrane at 80 V for 2 hours. Membranes were blocked using 5% dry milk in TBS at room temperature for 1 hour, washed with TBST, and then probed overnight at 4°C with the CM8E6 (1:500 in 5% milk in TBS) in-house antibody against MCV sT and the Sigma clone B-5-2-2 monoclonal mouse antibody against α-tubulin (1:10,000 in 5% milk in TBS) as a loading control. Membranes were washed with TBST and Licor 800 infrared dye-conjugated anti-mouse secondary antibody (1:10,000 in 5% milk in TBS) was then added for one hour at room temperature in the dark for visualization using a Licor Odyssey imager (**Figs 8-10**). MCV sT was observed in various tissues in mice harboring the UBC-ER-cre transgene and injected with tamoxifen, but not in UBC-ER-cre negative mice injected with tamoxifen nor UBC-ER-cre positive mice not injected with tamoxifen.

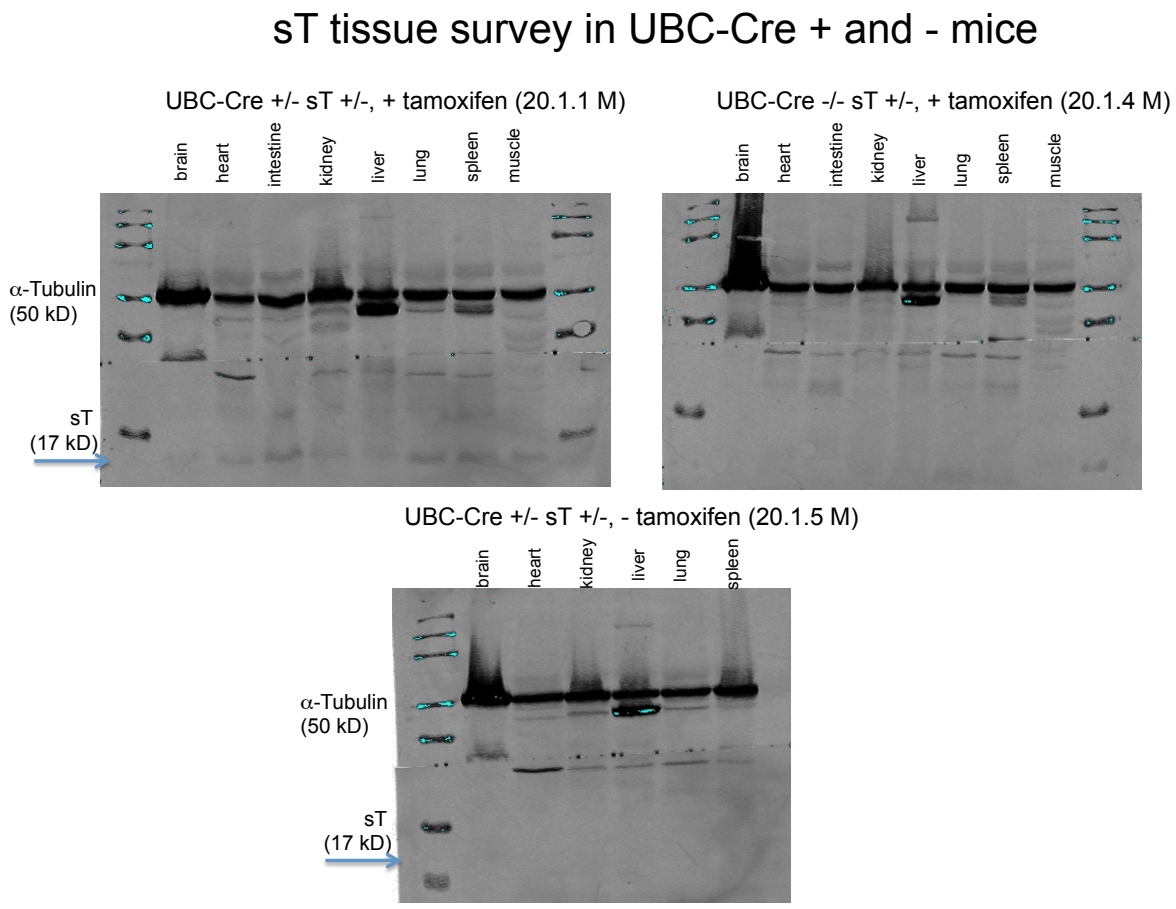

Figure 8. MCV sT and α-tubulin expression in various mice. MCV sT expression, at 17 kD, is only observed in mouse 20.1.1 M that harbors UBC-ER-cre and was injected with tamoxifen.

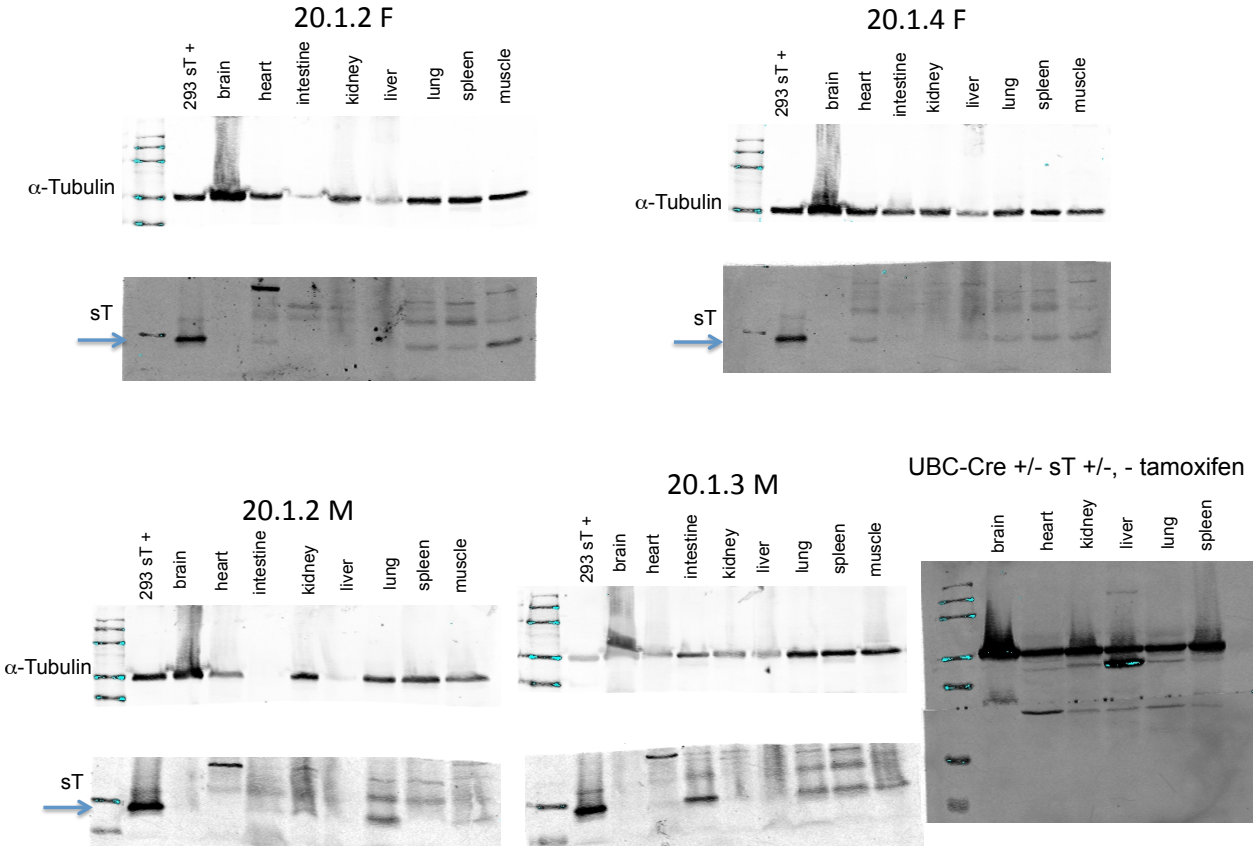

Figure 9. Western blots of other UBC-ER-cre positive mice injected with tamoxifen. MCV sT was observed in various tissues in these mice. No tamoxifen, cre positive negative control blot is also included.

5.5 TUNEL STAINING TO DETECT CELL DEATH IN TISSUE SAMPLES

Organ samples in 10% buffered formalin from a UBC-ER-cre positive mouse and a UBC-ER-cre negative mouse were sent to Research Histology Services at the University of Pittsburgh for paraffin embedding and slide preparation, TUNEL (terminal dUTP nick-end labeling) and hematoxylin/eosin staining. Increased cell death was observed in the intestine, lung, liver and spleen (**Figs 11-14**).

5.6 DISCUSSION

The purpose of the above experiments was to study the effects MCV sT *in vivo*. To do this, we crossed a transgenic MCV sT knock-in mouse developed by GenOway to UBC-ER-cre mice to derive progeny that express MCV sT in all tissues upon tamoxifen induction. Addition of tamoxifen resulted in dramatic weight loss, which necessitated eventual sacrifice, in offspring carrying the UBC-ER-cre transgene. Western blots of various tissue lysates detected MCV sT expression in these offspring. This indicates that tamoxifen addition successfully induced ER-cre translation into the nucleus and subsequent excision of the STOP cassette that had been blocking MCV sT expression. However, the connection between MCV sT expression and the dramatic weight loss observed remains obscure.

One possibility is increased cell death in response to MCV sT expression. TUNEL staining of UBC-ER-cre positive mouse tissue indicated significant cell death in the lung, liver, intestine and spleen compared to UBC-ER-cre negative mouse tissue. The drastic increase in viral oncogene expression may have severely deleterious effects on cellular

function, thus inducing a self-destructive cascade. Being that MCV sT is expressed systemically in UBC-ER-cre positive mice upon tamoxifen induction, such widespread cellular damage may promote organ failure, particularly in the intestines, which would disrupt nutrient uptake. This could account for the observed severe weight loss. However, the molecular mechanism by which induced MCV sT expression may result in cell death remains unknown, although possible experiments are proposed in section **6.1**.

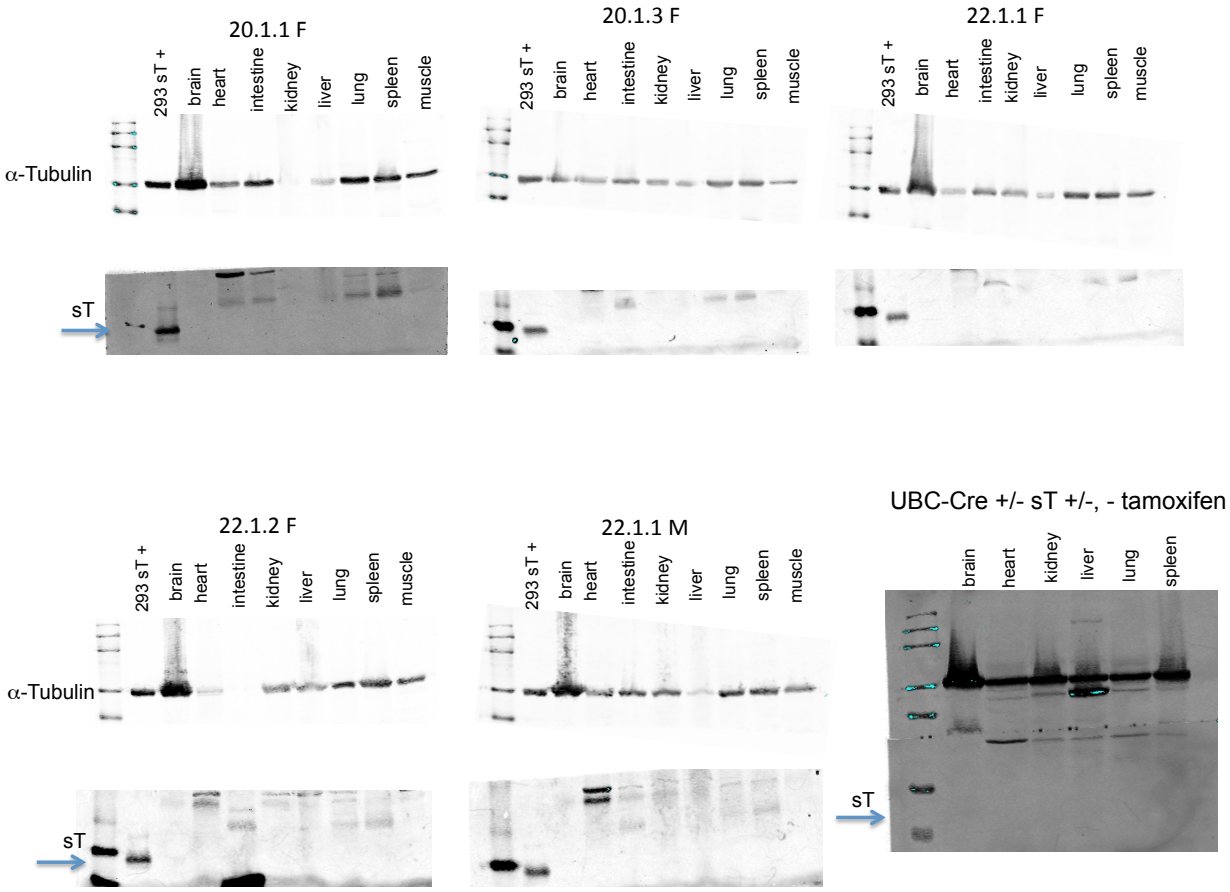

Figure 10. Western blots of other UBC-ER-cre negative mice injected with tamoxifen. MCV sT expression was not observed in these mice. No tamoxifen, cre positive negative control blot is also included.

Intestine

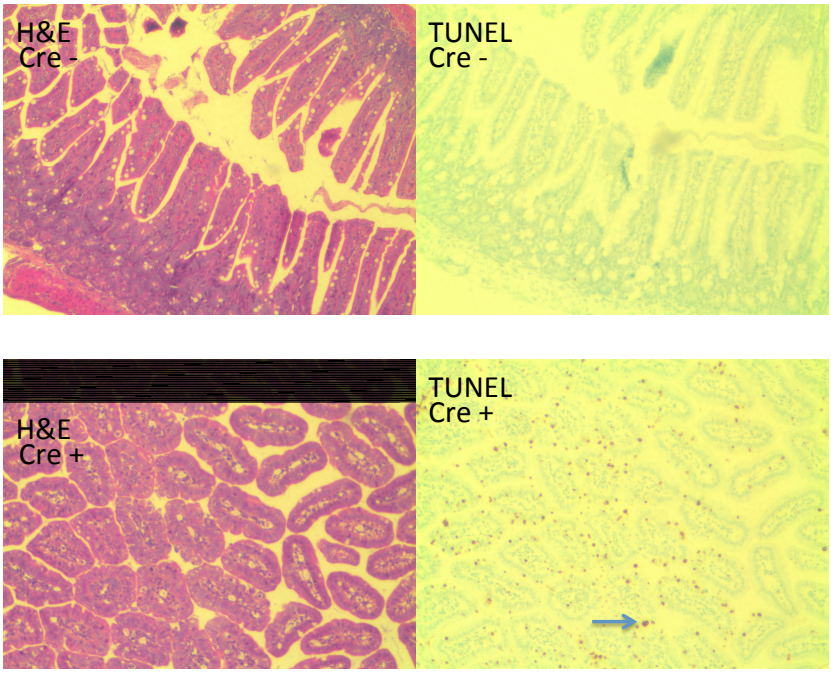

Figure 11. TUNEL and H&E staining of intestine from a cre positive and cre negative mouse. Increased TUNEL staining, and therefore cell death, is observed in the cre positive mouse. Arrow indicates a TUNEL positive cell.

Lung

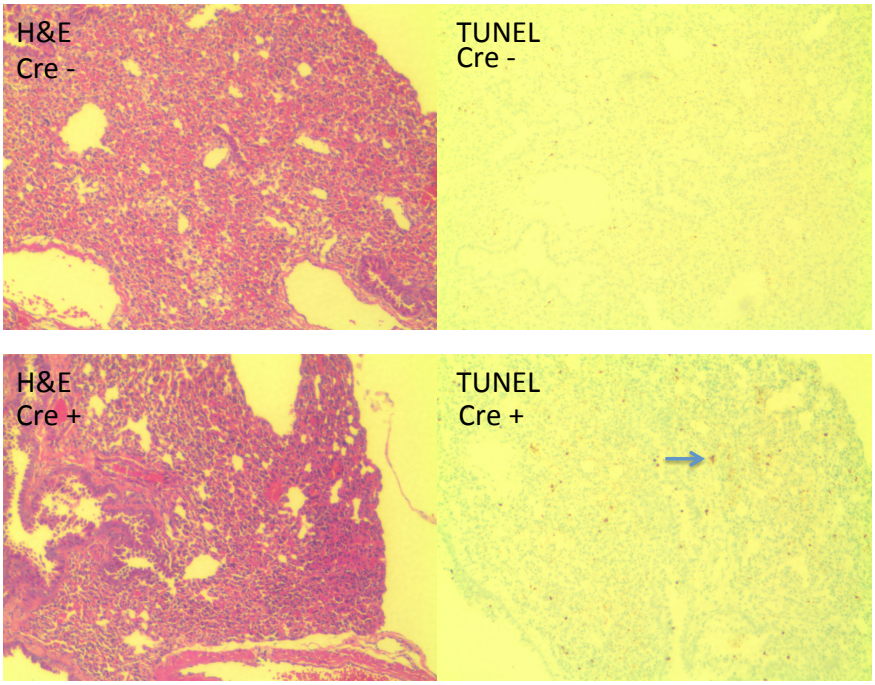

Figure 12. TUNEL and H&E staining of lung from a cre positive and cre negative mouse. Increased TUNEL staining, and therefore cell death, is observed in the cre positive mouse. Arrow indicates a TUNEL positive cell.

Liver

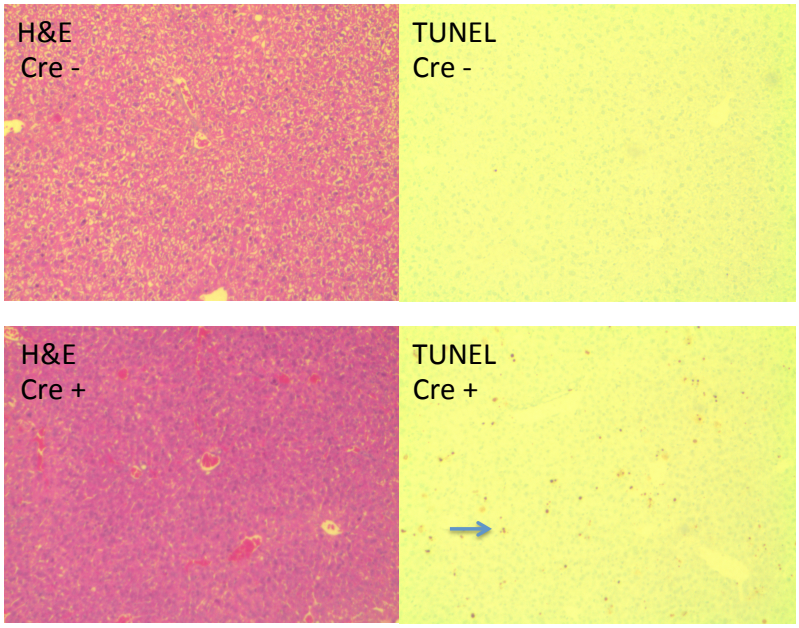

Figure 13. TUNEL and H&E staining of liver from a cre positive and cre negative mouse. Increased TUNEL staining, and therefore cell death, is observed in the cre positive mouse. Arrow indicates a TUNEL positive cell.

Spleen

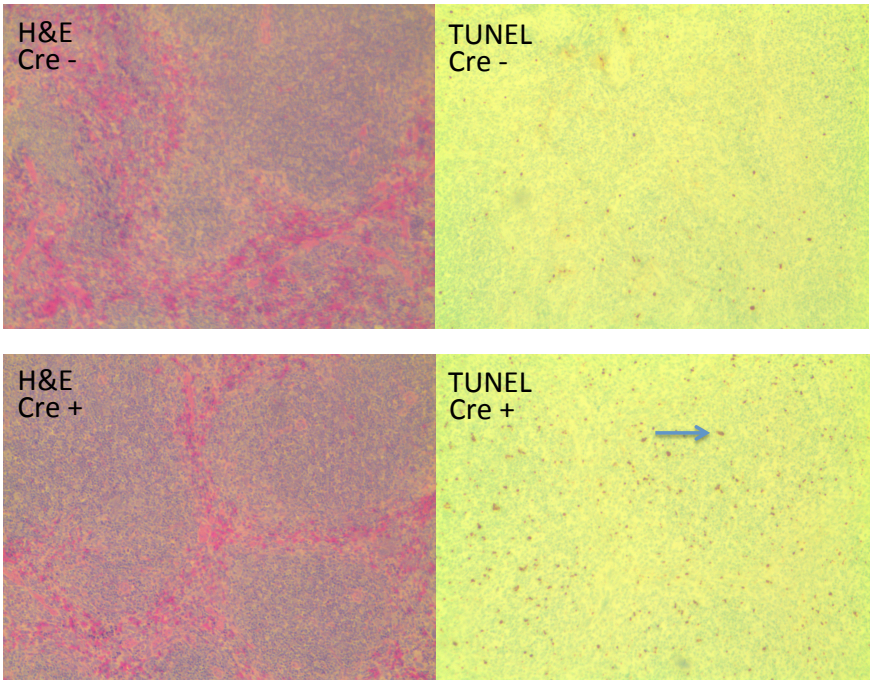

Figure 14. TUNEL and H&E staining of spleen from a cre positive and cre negative mouse. Increased TUNEL staining, and therefore cell death, is observed in the cre positive mouse. Arrow indicates a TUNEL positive cell.

6.0 FUTURE DIRECTIONS

6.1 EXPRESSION OF MOLECULAR MARKERS IN RESPONSE TO ST

As mentioned above, expression of MCV sT leads to hyperphosphorylation and inhibition of the cap-dependent translation inhibitor 4E-BP1, thus promoting increased cap-dependent translation, which may be a mechanism of transformation (21). It would therefore be of interest to determine whether there is an increase of 4E-BP1 hyperphosphorylation in tissues from UBC-ER-cre positive mice that express sT. This could be evaluated using western blotting against phosphorylated 4E-BP1. If tissues expressing sT display hyperphosphorylated 4E-BP1, it confirms that this mechanism is present *in vivo* as well as in an *in vitro* cell culture model, and thus is more relevant.

Being that cell death was observed in several tissues via TUNEL staining, it may also be worthwhile to determine whether these same tissues express markers of apoptosis using western blot. These could include cleaved PARP, caspase-3 cleavage, and a variety of the Bcl proteins. This would provide a possible mechanism by which sT induces cell death in specific tissues where it is expressed. Another marker could be upregulation of the tumor suppressor p53, which can also lead to apoptosis in response to transforming agents. If sT is such an agent, then it may induce activation of p53.

6.2 DECREASING THE DOSAGE OF TAMOXIFEN

Our dosage of 0.2 mg/g of tamoxifen used for injection led to the necessary sacrificing of all UBC-ER-cre positive mice due to weight loss. This dosage may have induced such a high amount of sT expression that it proved toxic to the mice. The cell death observed in the intestines may have been an indication of this toxicity; poor nutrient uptake in the intestines may have promoted the severe and sudden weight loss observed in these mice. The euthanizing of these mice prevented us from observing any tumor formation and thus this was not a valid model of cancer development. Therefore, using a lower dose of tamoxifen may induce lower amounts of sT expression and thus circumvent the cell death and weight loss. This would enable the mice to live longer and provide a better chance of observing any possible tumor formation. A good starting dosage may be 0.02 mg/g of tamoxifen, ten times less than our initial dosage. If this dosage also results in the weight loss and necessary sacrificing of UBC-ER-cre positive mice before tumor formation is observed, then the dosage could again be decreased to promote survival. A drawback to this experiment is that lower dosages of tamoxifen may not promote robust expression of sT in the mice, and thus no possible tumor formation will be observed.

6.3 USING CRE LINES DRIVEN BY DIFFERENT PROMOTERS

The ER-cre transgene we used in this experiment was under the control of the ubiquitin promoter, resulting in the expression of ER-cre in all tissues. When crossed to MCV sT transgenic mice and after translocation of ER-cre into the nucleus using tamoxifen injection, sT is expressed in multiple tissues, as observed in our western blots. This

widespread expression of sT may be toxic to the mice, thus resulting in the observed weight loss, cell death and necessary sacrificing. Accordingly, using different promoters to drive the cre transgene may be worthwhile. Being that MCC is specific to Merkel cells in the skin, using the Atoh1 promoter, which controls expression of the Atoh1 transcription factor in Merkel cells and the CNS, may be worthwhile (54). We attempted this using a constitutive Atoh1-cre line (B6.Cg-Tg(Atoh1-cre)1Bfri/J, Jackson Labs #011104) crossed to our MCV sT transgenic mice, but obtained no viable cre-positive pups according to PCR genotyping. This may indicate that constitutive expression of sT in the CNS is toxic to embryos. Another constitutive promoter we tried was that for keratin 14, a skin-specific structural protein (Tg(KRT14-cre)1Amc/J, Jackson Labs #004782)(55). However, this also produced no viable cre-positive pups. Despite these negative results, other promoters may still be of interest, such as for other skin-specific proteins. This would be the most relevant *in vivo* model given that MCC is a skin cancer.

BIBLIOGRAPHY

1. Toker C. Trabecular carcinoma of the skin. Arch Dermatol 1972; 105:107-10.

2. Chang M, Moore PS. Merkel Cell Carcinoma: A Virus-Induced Human Cancer. Annu Rev Pathol Mech Dis 2012; 7:123-44.

3. Sibley RK, Dehner LP, Rosai J. Primary neuroendocrine (Merkel cell?) carcinoma of the skin. I. a clinicopathologic and ultrastructural study of 43 cases. Am J Surg Pathol 1985; 9:95-108.

4. Hodgson NC. Merkel cell carcinoma: changing incidence trends. J Surg Oncol 2005; 89:1-4.

5. Angelli M, Clegg LX. Epidemiology of primary Merkel cell carcinoma in the United States. J Am Acad Dermatol 2003; 49:832-41.

6. Miller RW and Rabkin CS. Merkel cell carcinoma and melanoma: etiological similarities and differences. Cancer Epidemiol Biomarkers Prev 1999; 8:153-58.

7. Heath M, Jaimes N, Lemos B, Mostaghimi A, Wang LC, et al. Clinical characteristics of Merkel cell carcinoma at diagnosis in 195 patients: the AEIOU features. J Am Acad Dermatol 2008; 58:375-81.

8. Feng H, Shuda M, Chang Y, Moore PS. Clonal Integration of a Polyomavirus in Human Merkel Cell Carcinoma. Science 2008. ; 319:1096-1100.

9. Shuda M, Arora R, Kwun HJ, Feng H, Sarid R et al. Human Merkel cell polyomavirus infection I. MCV T antigen expression in Merkel cell carcinoma, lymphoid tissues and lymphoid tumors. Int J Cancer 2009; 125:1243-49.

10. Laude HC, Jonchere B, Maubec E, Carlotti A, Marinho E, et al. 2010. Distinct Merkel cell polyomavirus molecular features in tumour and non tumour specimens from matients with Merkel cell carcinoma. *PLoS Pathog.* 6:8.

11. Sastre-Garau X, Peter M, Avril MF, Laude H, Coutrier J, et al. Merkel cell carcinoma of the skin: pathological and molecular evidence for a causative role of MCV in oncogenesis. J Pathol 2009; 218:48-56.

12. Houben R, Shuda M, Weinkam R, Schrama D, Feng H, et al. Merkel cell polyomavirus-infected Merkel cell carcinoma cells require expression of viral T antigens. J Virol 2010; 84:7064-72.

13. Moore PS, Chang Y. Why do viruses cause cancer? Highlights of the first century of human tumour virology. Nat Rev Cancer 2010 ;10:878-89.

14. Schowalter RM, Pastrana DV, Pumphrey KA, Moyer AL, Buck CB. Merkel cell polyomavirus and two previously unknown polyomaviruses are chronically shed from human skin. Cell Host Microbe 2010; 7:509-15.

15. Carter JJ, Paulson KG, Wipf GC, Miranda D, Madeleine MM, et al. Association of Merkel cell polyomavirus-specific antibodies with Merkel cell carcinoma. J Natl Cancer Inst 2009; 95:1522-30.

16. Tolstov YL, Pastrana DV, Feng H, Becker JC, Jenkins FJ et al. Human Merkel cell polyomavirus infection. II. MCV is a common human infection that can be detected by conformational capsid epitope immunoassays. Int J Cancer 2009; 125:1250-56.

17. Shuda M, Feng H, Kwun HJ, Rosen ST, Gjoerup, et al. T antigen mutations are a human tumor-specific signature for Merkel cell polyomavirus. Proc Natl Acad Sci USA 2008; 110:209-17.

18. Kwun HJ, Guastafierro A, Shuda M, Meinke G, Bohm A, et al. The minimum replication origin of Merkel cell polyomavirus has a unique large T-antigen loading architecture and requires small T-antigen expression for optimal replication. J Virol 2009; 83:12118-28.

19. Kassem A, Schopflin A, Diaz C, Weyers W, Stickeler E, et al. Frequent detection of Merkel cell polyomavirus in human Merkel cell carcinomas and identification of a unique deletion in the VP1 gene. Cancer *Res* 2008; 68:5009-13.

20. Arora R, Chang Y, Moore PS. MCV and Merkel cell carcinoma: a molecular success story. Curr Op Virol 2012; 2:1-10.

21. Shuda M, Kwun HJ, Feng H, Chang Y, Moore PS. Human Merkel cell polyoma small T antigen is an oncoprotein targeting the 4E-BP1 translation regulator. J Clin Invest 2011; 121: 3623-34.

22. Houben R, Adam C, Baeurle A, Hesbacher S, Grimm J, et al. An intact retinoblastoma protein binding site in Merkel cell polyomavirus large T antigen is required for promoting growth of Merkel cell carcinoma cells. Int J Cancer 2011; 130:847-56.

23. Arora R, Shuda M, Guastafierro A, Feng H, Toptan T, Tolstov Y, et al. Survivin is a therapeutic target in Merkel cell carcinoma. Sci Trans Med 2012; 4:133-56.

24. Saenz-Robles MT, Pipas JM. T antigen transgenic mouse models. Sem Cancer Bio 2009; 19:229-35.

25. Chen J, Tobin GJ, Pipas JM, Van Dyke T. T-antigen mutant activities in vivo: roles of p53 and pRb binding in tumorigenesis of the choroid plexus. Oncogene 1992; 7(6):1167-75.

26. Chen JD, Van Dyke T. Uniform cell-autonomous tumorigenesis of the choroid plexus by papovavirus large T angtigens. Mol Cell Bio 1991; 11(12):5968-76.

27. Lee YC, Asa SL, Drucker DJ. Glucagon gene 5'-flanking sequences direct expression of simian virus 40 large Tantigen to the intestine, producing carcinoma of the large bowel in transgenic mice. J Biol Chem 1992; 267(15):10705-8.

28. Ratineu C, Ronco A, Leiter AB. Role of the amino-terminal domain of simian virus 40 early region in inducing tumors in secretin-expressing cells in transgenic mice. Gastroenterology 2000; 119(5):1305-11.

29. Upchurch BH, Fung BP, Rindi G, Ronco A, Leiter AB. Peptide YY expression is an early event in colonic endocrine cell differentiation: evidence from normal and transgenic mice. Development 1996; 122(4):1157-63.

30. Garabedian EM, Roberts LJ, McNevin MS, Gordon JI. Examining the role of Paneth cells in the small intestine by lineage ablation in transgenic mice. J Biol Chem 1997; 272(38): 23729-40.

31. Gum Jr JR, Hicks JW, Gillespie AM, Rius JL, Treseler PA, Kogan SC, et al. Mouse intestinal goblet cells expressing SV40 T antigen directed by the MUC2 mucin gene promoter undergo apoptosis upon migration to the villi. Cancer Res 2001l; 61(8):3472-9.

32. Herring BP, Hoggart AM, Smith AF, Gallagher PJ. Targeted expression of SV40 T large T-antigen to visceral smooth muscle induces proliferation of contractile smooth muscle cells and results in megacolon. J Biol Chem 1999; 274(25):17725-32.

33. Kim SH, Roth KA, Moser AR, Gordon JI. Transgenic mouse models that explore the multistep hypothesis of intestinal neoplasia. J Cell Biol 1993; 123(4): 877-93.

34. Kim SH, Roth KA, Coopersmith CM, Pipas JM, Gordon JI. Expression of wild-type and mutant simian virus 40 large tumor antigens in villus-associated enterocytes of transgenic mice. Proc Natl Acad Sci USA 1994; 91(15):6914-8.

35. Hauft SM, Kim SH, Schmidt GH, Pease S, Rees S, Harris S, et al. Expression of SV-40 T antigen in the small intestinal epithelium of transgenic mice results in proliferative changes in the crypt and reentry of villus-associated enterocytes into the cell cycle but has no apparent effect on cellular differentiation programs and does not cause neoplastic transformation. J Cell Biol 1992; 117(4): 825-39.

36. Markovics JA, Carroll PA, Robles MT, Pope H, Coopersmith CM, Pipas JM. Intestinal dysplasia induced by simian virus 40 T antigen is independent of p53. J Virol 2005; 79(12):7492-502.

37. Saenz-Robles MT, Markovics JA, Chong JL, Opavsky R, Whitehead RH, Leone G, et al. Intestinal hyperplasia induced by simian virus 40 large tumor antigen requires E2F2. J Virol 2007; 81(23):13191-9.

38. Chandresekaran C, Coopersmith CM, Gordon JI. Use of normal and transfenic mice to examine the relationship between terminal differentiation of intestinal epithelial cells and accumulation of their cell cycle regulators. J Biol Chem 1996; 271(45):28414-21.

39. Rathi AV, Saenz-Robles MT, Pipas JM. Enterocyte proliferation and intestinal hyperplasia induced by simian virus 40 T antigen require a functional J domain. J Virol 2007; 81(17):9481-9.

40. Windle JJ, Albert DM, O'Brien JM, Marcus DM, Disteche CM, Bernards R, et al. Retinoblastoma in transgenic mice. Nature 1990; 343(6259):665-9.

41. Mahon KA, Chepelinsky AB, Khillan JS, Overbeek PA, Piatigorsky J, Westphal H. Oncogenesis of the lens in transgenic mice. Science 1987; 235(4796):1622-8.

42. Chen Q, Liang D, Fromm LD, Overbeek PA. Inhibition of lens fiber cell morphogenesis by expression of a mutant SV40 large T antigen that binds CREB-binding protein/p300 but not pRb. J Biol Chem 2004; 279(17):17667-73.

43. Fromm L, Shawlot W, Gunning K, Butel JS, Overbeek PA. The retinoblastoma protein-binding region of simian virus 40 large T antigen alters cell cycle regulation in lenses of transgenic mice. Mol Cell Biol 1994; 14(10):6743-54.

44. Hanahan D. Heritable formation of pancreatic beta-cell tumors in transgenic mice expressing recombinant insulin/simian virus 40 oncogenes. Nature 1985; 315(6015):115-22.

45. Herzig M, Novatchkova M, Christofori G. An unexpected role for p53 in augmenting SV40 large T antigen-mediated tumorigenesis. Biol Chem 1999; 380(2):203-11.

46. Christofori G, Naik P, Hanahan D. A second signal supplied by insulin-like growth factor II in oncogene-induced tumorigenesis. Nature 1994; 369(6479):414-8.

47. Ornitz DM, Hammer RE, Messing A, Palmiter RD, Brinster RL. Pancreatic neoplasia induced by SV40 T-antigen expression in acinar cells of transgenic mice. Science 1987; 238(4824):188-93.

48. Bell Jr RH, Memoli VA, Longnecker DS. Hyperplasia and tumors of the islets of Langerhans in mice bearing an elastase I-SV40 T-antigen fusion gene. Carcinogenesis 1990; 11(8):1393-8.

49. Ceci JD, Kovatch RM, Swing DA, Jones JM, Snow CM, Rosenberg MP, et al. Transgenic mice carrying a murine amylase 2.2/SV40 T antigen fusion gene develop pancreatic acinar cell and stomach carcinomas. Oncogene 1991; 6(2):323-32.

50. Ramel S, Sanchez CA, Schimke MK, Neshat K, Cross SM, Raskind WH, et al. Inactivation of p53 and the development of tetraploidy in the elastase-SV40 T antigen transgenic mouse pancreas. Pancreas 1995; 11(3):213-22.

51. Tevethia MJ, Bonneau RH, Griffith JW, Mylin A. A simian virus 40 large T-antigen segment containing amino acids 1 to 127 and expressed under the control of the rat elastase-1 promoter priduces pancreatic acinar carcinomas in transgenic mice. J Virol 1997; 71(11):8157-66.

52. Friedrich G, Soriano P. Promoter traps in embryonic stem cells: a genetic screen to identify and mutate developmental genes in mice. Genes Dev 1991; 5(9):1513-23.

53. Zambrowicz BP, Imamoto A, Fiering S, Herzenberg LA, Kerr WG, Soriano P. Disruption of overlapping transcripts in the ROSA beta geo 26 gene trap strain leads to widespread expression of beta-galactosidase in mouse embyos and hematopoietic cells. Proc Natl Acad Sci USA 1997. 94(8):3789-94.

54. Mulvaney J, Daboub A. Atoh1, an Essential Transcription Factor in Neurogenesis and Intestinal and Inner Ear Development: Function, Regulation and Context Dependency. JARO 2012; 13:281-293.

55. Coulombe PA, Lee CH. Defining Keratin Protein Function in Skin Epithelia: Epidermolysis Bullosa Simplex and Its Aftermath. J Inv Dermat 2012; 132:763-775.